Acta Crystallographica Section F
**Structural Biology and Crystallization Communications**
ISSN 1744-3091

# Purification, crystallization and preliminary X-ray diffraction analysis of the effector protein PevD1 from *Verticillium dahliae*

**Lei Han,[a] Zheng Liu,[a] Xinqi Liu[b] and Dewen Qiu[a]***

[a]Key Laboratory of Integrated Pest Management in Crops, Ministry of Agriculture, Institute of Plant Protection, Chinese Academy of Agricultural Sciences, 12 Zhongguancun South Street, Beijing 100081, People's Republic of China, and [b]State Key Laboratory of Medicinal Chemical Biology, College of Life Sciences, Nankai University, Tianjin 300071, People's Republic of China

Correspondence e-mail: qiudewen@caas.net.cn

Received 7 March 2012
Accepted 7 May 2012

The effector protein PevD1 from the pathogenic fungus *Verticillium dahliae* was purified and crystallized using the hanging-drop vapour-diffusion method. Native crystals appeared in a solution consisting of 4.0 *M* sodium formate. A native data set was collected at 1.9 Å resolution at 100 K using an in-house X-ray source. Because of the absence of useful methinione in the protein sequence, derivative crystals that contained iodine were obtained by soaking in 1.25 *M* potassium iodide, and a data set that contained anomalous signal was collected using the same X-ray facility at a wavelength of 1.54 Å. The single-wavelength anomalous dispersion method was used to successfully solve the structure based on the anomalous signal generated from iodine.

## 1. Introduction

Plants are exposed to various pathogens during their life cycle. Over many years of evolution, plants have developed a set of tactics to recognize and fight various pathogens, including viruses, bacteria and fungi, through a mechanism termed innate immunity (Boller & He, 2009). Two pathways have been reported to be involved in plant innate immunity. One is induced by pathogen-associated or microbial-associated molecular patterns (PAMPs or MAMPs), such as flagellin FLS2 (Zipfel & Felix, 2005), and is recognized by transmembrane pattern-recognition receptors (PRRs). These responses are referred to as PAMP-triggered immunity (PTI). The other defence system is called effector-triggered immunity (ETI) and acts largely inside the cell. The effectors secreted by pathogens to suppress PTI are recognized by another type of receptor (NB-LRR) that shares typical nucleotide-binding (NB) and leucine-rich repeat (LRR) domains. The pathogens secrete a series of elicitors/effectors to regulate plant physiology for the benefit of self-growth. Plants can recognize pathogen elicitors/effectors and emit multifaceted downstream signals to control the exploitation of pathogens. The balance between plants and pathogens drives the co-evolution of the two kingdoms (Boller & He, 2009; Jones & Dangl, 2006).

PevD1, a novel effector protein from the pathogenic cotton wilt fungus *Verticillium dahliae*, is able to trigger a hypersensitive response in tobacco plants. It was isolated from the culture medium of the fungus and analyzed by *de novo* sequencing. The PevD1 gene consists of 468 bp encoding 155 amino-acid residues with a theoretical molecular weight of 16.23 kDa. A *BLAST* search against the nonredundant sequence database showed that this gene is identical to the genomic sequence of a putative protein from *V. dahliae* strain VdLs. 17 (GenBank accession No. ABJE 01000445.1), the function of which remains unknown. Our previous experiments showed that recombinant PevD1-treated tobacco plants exhibited enhanced systemic acquired resistance, which was reflected by a significant reduction in the number and size of TMV lesions on tobacco leaves. A further study of PevD1-treated leaves of tobacco plants showed that the protein can induce hydrogen peroxide, extracellular-medium alkalization, callose deposition, phenolic metabolism and lignin synthesis (Wang *et al.*, 2012). These resistance responses are well known to be activated on infection by a large spectrum of pathogens

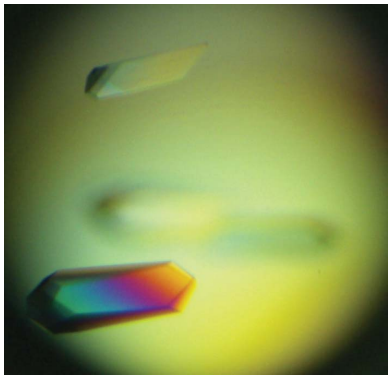

(Garcia-Brugger *et al.*, 2006). However, the mechanism that underlies these functions remains unclear.

In order to study the molecular mechanism of PevD1 from a structural basis, PevD1 was expressed and crystallized. A set of high-resolution native data was successfully collected using an in-house X-ray source. As there is no homologous structure for solution of the phase problem, iodine-derivative data sets for structure determination were collected using a similar procedure.

## 2. Materials and methods

### 2.1. Cloning

The full-length PevD1 gene (GenBank accession No. HQ540585.1) consists of 468 bp encoding 155 residues. The first 18 residues were predicted to be a secretory signal using the *SignalP* 3.0 server (Bendtsen *et al.*, 2004). The sequence without the signal peptide, encoding amino acids 19–155, was cloned into the pET30-TEV/LIC vector (Novagen) downstream of a 6×His tag. The forward primer 5′-TACTTCCAATCCAATGCCGCCCCCGCGTCTCCCGGC-3′ and the reverse primer 5′-TTATCCACTTCCAATGCTAAGCCTCG-GCGGGAGCGTC-3′ were used to amplify the sequence. The polymerase chain reaction (PCR) program was as follows: 367 K for 7 min, 28 cycles of 367 K for 40 s, 331 K for 40 s and 345 K for 40 s, and a final extension at 345 K for 10 min. The PCR product was then cloned into the vector using ligation-independent cloning (Aslanidis & de Jong, 1990).

### 2.2. Expression and purification

The recombinant expression vector was transformed into *Escherichia coli* Codon Plus competent cells. The cells were grown in LB

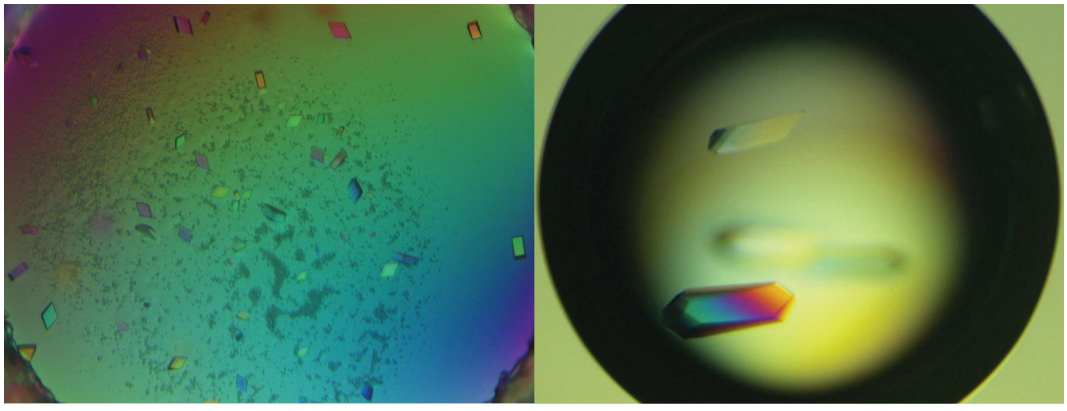

(*a*) (*b*)

**Figure 1**
(*a*) Crystals grown in 0.1 *M* HEPES pH 7.5, 1.4 *M* sodium citrate tribasic dehydrate. The approximate dimensions of the crystals are 50 × 50 × 20 µm. (*b*) Crystals grown in 3.8 *M* sodium formate. The approximate dimensions of the crystals are 500 × 500 × 1500 µm.

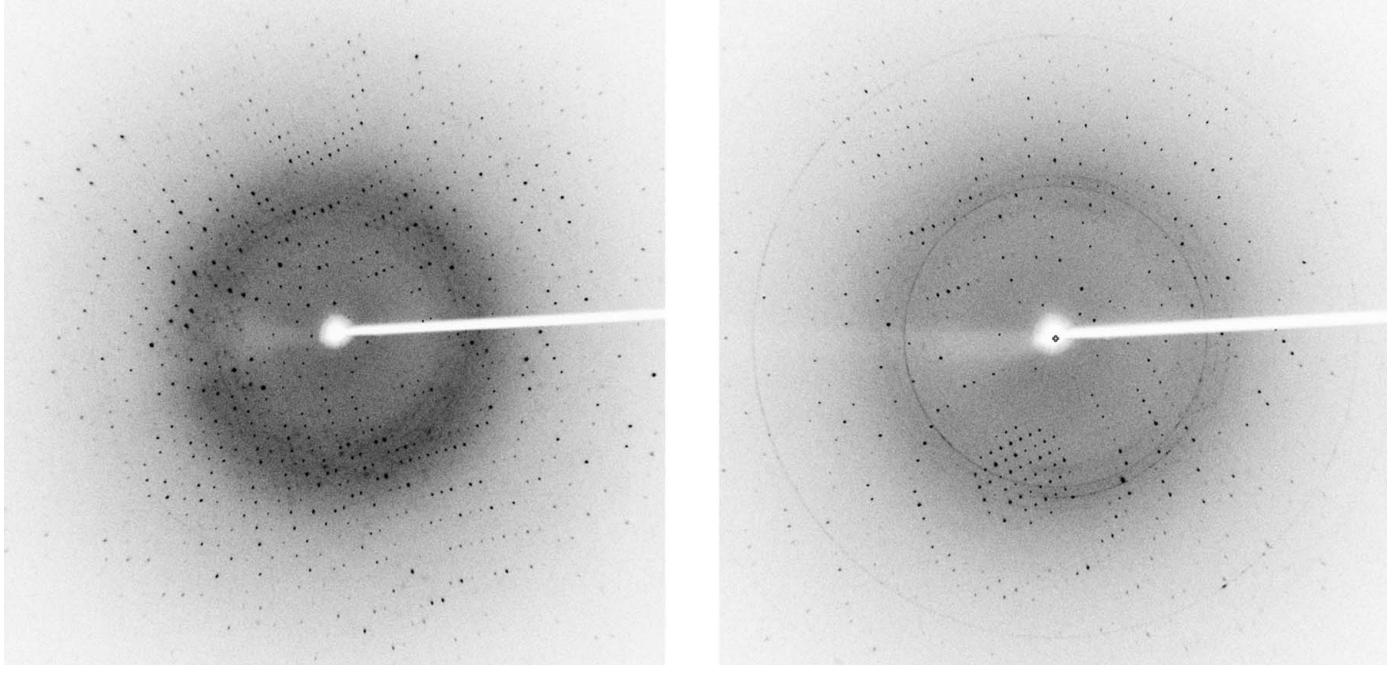

**Figure 2**
Diffraction patterns of PevD1 crystals.

**Table 1**
Data-collection and processing statistics.

Values in parentheses are for the outer resolution shell.

| Data set | Native | Iodine derivative |
|---|---|---|
| X-ray source | Rigaku MicroMax-007 HF | Rigaku MicroMax-007 HF |
| Wavelength (Å) | 1.5418 | 1.5418 |
| Detector | R-AXIS HTC image plate | R-AXIS HTC image plate |
| Crystal parameters | | |
| Space group | $C222_1$ | $C222_1$ |
| Unit-cell parameters | | |
| $a$ (Å) | 58.00 | 59.38 |
| $b$ (Å) | 79.49 | 78.58 |
| $c$ (Å) | 55.51 | 55.36 |
| $\alpha$ (°) | 90 | 90 |
| $\beta$ (°) | 90 | 90 |
| $\gamma$ (°) | 90 | 90 |
| Resolution (Å) | 50–1.9 (2.04–1.90) | 50–2.1 (2.29–2.10) |
| Mosaicity (°) | 0.35 | 0.73 |
| Solvent content (%) | 48.13 | 48.61 |
| Molecules per asymmetric unit | 1 | 1 |
| Data processing | | |
| No. of observed reflections | 72474 (3537) | 50521 (2258) |
| No. of unique reflections | 11146 (558) | 8009 (367) |
| Completeness (%) | 98.6 (95.3) | 98.2 (92.7) |
| Multiplicity | 6.5 (6.4) | 6.3 (5.9) |
| $R_{\rm merge}$† (%) | 4.3 (10.6) | 8.6 (17.5) |
| Average $I/\sigma(I)$ | 15.7 (3.1) | 13.9 (2.7) |

† $R_{\rm merge} = \sum_{hkl}\sum_i |I_i(hkl) - \langle I(hkl)\rangle| / \sum_{hkl}\sum_i I_i(hkl)$, where $\langle I(hkl)\rangle$ is the mean intensity of the $i$ observations of symmetry-related reflections of $hkl$.

medium at 310 K to an $OD_{600}$ of 0.6 and then induced with 0.1 m*M* IPTG for 12 h at 289 K. The cells were harvested by centrifugation at 5000*g* for 15 min. The sedimented cells were resuspended in Ni–IMAC matrix binding buffer (25 m*M* Tris, 300 m*M* NaCl pH 8.0) and disrupted by sonication. After centrifugation at 18 000*g* for 40 min, the supernatant was loaded onto an Ni–IMAC matrix column and washed with washing buffer (binding buffer plus 10 m*M* imidazole). Finally, the protein was eluted using elution buffer (binding buffer plus 200 m*M* imidazole). For further purification, the protein was concentrated and diluted with a low-salt buffer (25 m*M* Tris pH 8.0). Ion-exchange chromatography was performed using a linear NaCl elution gradient from 0 to 1 *M* with a HiTrap Q HP column (GE Healthcare). The eluted peak was loaded onto a HiLoad 16/60 Superdex 200 size-exclusion column (GE Healthcare) in 25 m*M* Tris, 200 m*M* NaCl pH 8.0 for the last purification step. The target protein PevD1 with an extra 24 N-terminal residues was concentrated for further use.

### 2.3. Crystallization

Index, Crystal Screen and Crystal Screen 2 kits from Hampton Research were used for initial screening at 289 K using the sitting-drop vapour-diffusion method. The concentration of His-tagged PevD1 in the drops was 2 mg ml$^{-1}$. 1 µl protein solution was manually mixed with 1 µl reservoir solution in the drop and equilibrated against 80 µl reservoir solution. After approximately one month, two types of crystals were obtained during the initial screening (Fig. 1). One type was grown in Index condition No. 20 (0.1 *M* HEPES pH 7.5, 1.4 *M* sodium citrate tribasic dihydrate). The other type appeared in Crystal Screen condition No. 33 (4.0 *M* sodium formate). A further experiment showed that the latter crystal had much better diffraction quality than the former crystal. The latter crystallization condition was then optimized by slightly modifying the concentrations of both the precipitant and protein. Finally, well diffracting crystals were obtained from an optimized precipitant concentration of 3.8 *M* sodium formate with a protein concentration of 2 mg ml$^{-1}$. These optimized crystals grew to at least 200 × 200 × 200 µm within one week and yielded a good diffraction pattern (Fig. 2).

To solve the phasing problem, derivative crystals were obtained by soaking in a potassium iodide solution. After many trials, the optimal condition (1.25 *M* potassium iodide, 3.5 *M* sodium formate) for soaking was determined. A short soaking time of up to 5 min produced stable and reproducible derivative crystals.

### 2.4. Data collection and processing

Data collection was performed at 100 K at a wavelength of 1.54 Å using an in-house Rigaku MicroMax-007 HF X-ray source at Nankai University. Prior to data collection, the crystal was soaked for several seconds in a cryoprotectant composed of reservoir solution plus 20% glycerol. The crystal was then mounted on the beamline in a loop and flash-cooled in a nitrogen-gas stream at 100 K. Both the native and derivative data sets were collected at a wavelength of 1.54 Å using an R-AXIS HTC image plate. The crystal-to-detector distance was 160 mm. The oscillation angle was 1.0° and 180 images were collected.

All of the data sets were indexed, integrated and scaled with the *HKL*-2000 package (Otwinowski & Minor, 1997). The crystals belonged to space group $C222_1$, with one monomer per asymmetric unit. Data-collection statistics are shown in Table 1. Structure determination and associated functional experiments are in progress.

## 3. Discussion

In this paper, we expressed and crystallized PevD1, an effector protein from *V. dahliae*. The crystals showed strong diffraction quality and had a Matthews coefficient of 2.37 Å$^3$ Da$^{-1}$ (solvent content of 48.13%).

Mature PevD1 contains only one methionine residue, which is located in the flexible N-terminus. An attempt to solve the structure using the single-wavelength anomalous dispersion method by selenomethionine substitution failed because of weak anomalous signal in the derivative data set. To solve the phasing problem, iodide-derivative crystals were obtained by soaking in a potassium iodine solution. Because of the high quality of the protein crystals, several sets of high-quality data were collected from iodine-containing crystals. Using the *SHELX* program (Sheldrick, 2008), 12 I atoms were identified within one protein molecule and the iodine coordinates thus obtained were input into *PHENIX* (Adams *et al.*, 2010) for further phase determination. An interpretable electron-density map was then obtained and further refinement is under way.

Many plant pathogens secrete toxins that enhance microbial virulence by killing host cells. For example, many fungal and oomycete species induce necrosis and ethylene-inducing peptide 1 (Nep1)-like proteins (NLPs) that trigger leaf necrosis and immunity-associated responses in various plants. PevD1 is a newly identified fungal toxin from *V. dahliae*. Although many fungal toxins have been reported, the three-dimensional structures of these toxins have not been fully studied. Only a few structures, including that of an NLP (Ottmann *et al.*, 2009), have been reported. Therefore, the solution of the structures of these toxins and the comparison of their detailed mechanisms in regulation of the plant immune response are of great interest and will provide insights into the control of fungal diseases in critical plants such as cotton and rice.

This research was supported by the National Basic Research Program of China (973 Program; grants 2010CB911800 and 2011CB100700) and the National S&T Major Project on Major

Infectious Diseases (grant 2012ZX10001-008) from the Ministry of Science and Technology of the People's Republic of China.

## References

Adams, P. D. *et al.* (2010). *Acta Cryst.* D**66**, 213–221.
Aslanidis, C. & de Jong, P. J. (1990). *Nucleic Acids Res.* **18**, 6069–6074.
Bendtsen, J. D., Nielsen, H., von Heijne, G. & Brunak, S. (2004). *J. Mol. Biol.* **340**, 783–795.
Boller, T. & He, S. Y. (2009). *Science*, **324**, 742–744.
Garcia-Brugger, A., Lamotte, O., Vandelle, E., Bourque, S., Lecourieux, D., Poinssot, B., Wendehenne, D. & Pugin, A. (2006). *Mol. Plant Microbe Interact.* **19**, 711–724.
Jones, J. D. & Dangl, J. L. (2006). *Nature (London)*, **444**, 323–329.
Ottmann, C., Luberacki, B., Küfner, I., Koch, W., Brunner, F., Weyand, M., Mattinen, L., Pirhonen, M., Anderluh, G., Seitz, H. U., Nürnberger, T. & Oecking, C. (2009). *Proc. Natl Acad. Sci. USA*, **106**, 10359–10364.
Otwinowski, Z. & Minor, W. (1997). *Methods Enzymol.* **276**, 307–326.
Sheldrick, G. M. (2008). *Acta Cryst.* A**64**, 112–122.
Wang, B., Yang, X., Zeng, H., Liu, H., Zhou, T., Tan, B., Yuan, J., Guo, L. & Qiu, D. (2012). *Appl. Microbiol. Biotechnol.* **93**, 191–201.
Zipfel, C. & Felix, G. (2005). *Curr. Opin. Plant Biol.* **8**, 353–360.